Metallophysics and Advanced Technologies
Металофіз. новітні технол.
Metallofiz. Noveishie Tekhnol.
2019, vol. 41, No. 6, pp. 751–764
https://doi.org/10.15407/mfint.41.06.0751
Reprints available directly from the publisher

STRUCTURE AND PROPERTIES OF NANOSCALE AND MESOSCOPIC MATERIALS

PACS numbers: 07.07.Df, 68.65.Ac, 73.21.-b, 77.55.-g, 78.67.Pt, 87.80.-y

Optimization of Optical Parameters of Metal-Dielectric Heterostructures for Plasmonic Sensors Formation

L. V. Poperenko, A. L. Yampolskiy, O. V. Makarenko, and O. I. Zavalistyi

Taras Shevchenko National University of Kyiv,
60 Volodymyrska Str.,
UA-01033 Kyiv, Ukraine

Angular dependences of ellipsometric parameters ψ and Δ at external reflection as well as an internal reflection coefficient are experimentally measured for hybrid structures based on thin Au, Ag or Cu films protected by dielectric layers HfO_2 or MgF_2. Using numerical matrix method, appropriate angular dependences for such multilayer systems are calculated. Despite of the differences obtained at modelling of optical parameters of the objects between the ordinary (external reflection) and plasmonic (internal reflection) modes, the theoretical results are in good agreement with the experimental data. Angular positions of plasmonic attenuated internal reflection minima in Kretschmann geometry for the samples are calculated as functions of a refractive index n of a substance deposited onto appropriate samples. The shift of these minima is practically the same for each of the structures studied and amounts about of 100 deg/RIU in the vicinity of $n = 1.20$. This allows one to estimate the performance of given heterostructures functioning as sensors grounded on the effect of surface plasmon resonance.

Key words: multilayer structures, dielectric layer, ellipsometry, surface plasmon, biosensors.

Експериментально виміряно кутові залежності еліпсометричних параметрів ψ і Δ при зовнішньому відбиванні і коефіцієнта внутрішнього відбивання світла для гібридних структур на основі тонких плівок Au, Ag або Cu, захищених діелектричними шарами HfO_2 або MgF_2. За допомогою ма-

Corresponding author: Oleksii Volodymyrovych Makarenko
E-mail: almakar@univ.kiev.ua

Citation: L. V. Poperenko, A. L. Yampolskiy, O. V. Makarenko, and O. I. Zavalistyi, Optimization of Optical Parameters of Metal-Dielectric Heterostructures for Plasmonic Sensors Formation, *Metallofiz. Noveishie Tekhnol.*, **41**, No. 6: 751–764 (2019), DOI: 10.15407/mfint.41.06.0751.

тричного методу для зазначених багатошарових систем розраховано відповідні кутові залежності. Незважаючи на відмінності, отримані при моделюванні оптичних характеристик зразків між звичайним (зовнішнє відбивання) та поляритонним (внутрішнє відбивання) режимами, теоретичні результати добре узгоджуються з експериментальними даними. Обчислено кутові положення плазмонних мінімумів коефіцієнта внутрішнього відбивання у геометрії Кречмана для всіх зразків в залежності від показника заломлення n речовини, нанесеної на відповідну багатошарову структуру. Величина зсуву цих мінімумів практично однакова для всіх досліджених структур і складає близько 100° на одиницю приросту n в околі $n = 1{,}20$. Це дозволяє оцінити ефективність даних структур в якості сенсорів, що функціонують на ефекті збудження поверхневого плазмонного резонансу.

Ключові слова: багатошарові структури, діелектричний шар, еліпсометрія, поверхневі поляритони, біосенсори.

Экспериментально измерены угловые зависимости эллипсометрических параметров ψ и Δ при внешнем отражении и коэффициента внутреннего отражения света для гибридных структур на основе тонких плёнок Au, Ag или Cu, защищённых диэлектрическими слоями HfO_2 или MgF_2. С помощью матричного метода для указанных многослойных систем рассчитаны соответствующие угловые зависимости. Несмотря на различия, полученные при моделировании оптических характеристик образцов между обычным (внешнее отражение) и поляритонным (внутреннее отражение) режимами, теоретические результаты хорошо согласуются с экспериментальными данными. Вычислены угловые положения плазмонных минимумов коэффициента внутреннего отражения в геометрии Кречмана для всех образцов в зависимости от показателя преломления n вещества, нанесённого на соответствующую многослойную структуру. Величина смещения этих минимумов практически одинакова для всех исследованных структур и составляет около 100° на единицу прироста n в окрестности $n = 1{,}20$. Это позволяет оценить эффективность данных структур в качестве сенсоров, функционирующих на эффекте возбуждения поверхностного плазмонного резонанса.

Ключевые слова: многослойные структуры, диэлектрический слой, эллипсометрия, поверхностные поляритоны, биосенсоры.

(Received April 4, 2019; in final version, May 20, 2019)

1. INTRODUCTION

Biosensors based on surface plasmon resonance (SPR) are widely used in various fields of chemistry and biotechnology, for example, for sensing antibodies in solution [1]. SPR sensing has established itself as an important tool in the characterization of biomolecular interactions [2, 3]. However, a key limitation which has stunted a full development of high-performance SPR-based sensors is typical large losses associated

with constituent metals. Although gold has been known as the highest quality plasmonic material for the visible and near infrared applications, its usage has been limited due to practical issues of continuous thin film formation, stability, adhesion, and surface roughness. Another limitation of gold is the strong interband transitions that occur in the blue and green spectral regions (which give rise to its orange-yellow colour).

In general, metals with high free electron densities and few or no interband transitions are the strongest candidates for plasmonic metals. According to these criteria silver is the best candidate for plasmonics since it has the highest conductivity of any metal and very weak interband transitions in the visible. However, its reactivity in ambient conditions causes it to oxidize relatively quickly [4], limiting long-term device applications. Copper also has appropriate potential to produce in some aspects higher-quality plasmon resonances than gold in approximately the same spectral region [5]. Furthermore, copper is considerably cheaper than both the gold and silver [4]. However, copper oxidizes much more rapidly than either gold or silver [4, 6], leading to rapid deterioration of its plasmon resonance response [6].

In the present study, we propose a decision to the abovementioned challenge by using HfO_2 very thin layer as a protection of the copper/silver plasmonic film to prevent their oxidation in the air atmosphere and improve the SPR. It was chosen HfO_2 as a dielectric layer because of its very stable chemical behaviour and high refractive index about of $\approx 1.9–2.0$ in the visible [7]. Dielectric coating on top of plasmonic film acts as a high protective layer maintaining and enhancing the plasmonic properties of the combined structures at the same time. The aim of this work is to determine optical parameters of such heterostructures layers and estimate their SPR-response, in dependence on the used metal layer type. This helps to find optimal configuration for their functioning as plasmonic sensors.

2. EXPERIMENT

The samples, examined in this work, were prepared by electron beam evaporation method. They are 1 mm glass plates with thin metal (Au, Ag, and Cu) and dielectric (HfO_2, MgF_2) layers, sputtered onto their surface. To improve the bottom layer adhesion to the substrate, a thin intermediate Cr layer (1–3 nm) was been deposited as a fundament for all subsequent ones. The thickness of each layer was monitored by Quartz Crystal Microbalance (QCM) during deposition process. A set of the samples was been fabricated on the base of gold, or silver or copper, the structure of which is specified in Table 1. For comparison, one can briefly estimate the skin-layer thickness as $\delta = l/(4\pi k)$. It amounts 12–

TABLE 1. The structure of the samples and their parameters n and k determined at $\lambda = 625$ nm.

Sample No.	Material (nm)	Ellipsometry		Ellipsometry by Δ		Plasmon excitation	
		n	k	n	k	n	k
1	Cr (1.5)	3.155*	3.308*	3.155*	3.308*	3.155*	3.308*
	Au (47)	0.04	3.25	0.153	2.82	0.15–0.54	3.24–3.34
2	Cr (2)	3.155*	3.308*	3.155*	3.308*	3.155*	3.308*
	Au (40)	0.04	1.8–2.5	0.153	3.522	0.15–0.54	3.25–3.34
	HfO_2 (30)	2.107*	0.00*	2.107*	0.00*	2.107*	0.00*
3	Cr (2)	3.155*	3.308*	3.155*	3.308*	3.155*	3.308*
	HfO_2 (5)	2.107*	0.00*	2.107*	0.00*	2.107*	0.00*
	Au (40)	0.04	2.69	0.153	2.69	0.06	2.85
	HfO_2 (5)	2.107*	0.00*	2.107*	0.00*	2.107*	0.00*
	Au (10)	0.04	2.69	0.153	2.69	0.06	2.85
4	Cr (1.5)	3.155*	3.308*	3.155*	3.308*	3.155*	3.308*
	Ag (30)	0.04	3.98	0.04	3.98	0.60	3.33
	MgF_2 (30)	1.421*	0*	1.421*	0*	1.421*	0*
	Au (25)	0.22	2.94	0.22	2.94	0.53	2.77
5	Cr (1.5)	3.155*	3.308*	3.155*	3.308*	3.155*	3.308*
	Ag (45)	0.04	4.1	0.05	3.55	0.00–0.60	3.78–3.95
	HfO_2 (7)	2.107*	0.00*	2.107*	0.00*	2.00–2.25	0.00*
6	Cr (1.5)	3.155*	3.308*	3.155*	3.308*	3.155*	3.308*
	Ag (45)	0.01	4.6	0.05	3.86	0.07–0.21	4.02–4.05
	HfO_2 (8)	2.107*	0.00*	2.107*	0.00*	2.107*	0.00*
7	Cr (3)	3.155*	3.308*	3.155*	3.308*	3.155*	3.308*
	Cu (35)	0.113	3.484	0.113	3.484	0.17–0.27	3.24
	HfO_2 (10)	2.107*	0.00*	2.107*	0.00*	2.107*	0.00*
8	Cr (1.5)	3.155*	3.308*	3.155*	3.308*	3.155*	3.308*
	Cu (43)	0.04	4.16	0.113	3.24	0.06–0.55	3.26–3.37
	HfO_2 (7)	2.107*	0.00*	2.107*	0.00*	2.107*	0.00*

*Literary values.

14 nm at $\lambda = 625$ nm for the noble metals employed.

The samples 3 and 4 were obtained to excite a plasmon resonance in two metal films, which may provide a modified shape of the resonance

curve and enhance the overall absorption. Note that for the structures with a gold film, the protective dielectric layer is not obligatory, since gold does not tend to oxidize in the air ambient.

The data on the substrate refractive index n of the substrate glass was checked by recording the Brewster minimum of the reflection coefficient for p-polarized light. Obtained $n = 1.506 \pm 0{,}047$ at $\lambda = 625$ nm.

To control optical parameters of the layers (refractive index n and extinction coefficient k), there was performed an ellipsometric experiment and investigated surface plasmons excitation in them as well. Measurements were conducted on automated goniopolarimetric installation, previously mentioned in [8]. The control of the measurement process, as well as the numerical processing of the results obtained, was carried out with the help of the programs we developed in LabView environment. The given installation allowed to solve a wide class of experimental problems related to the measurement of angular distributions of intensity and polarization state of optical radiation, in particular, reflected from the investigated heterostructures.

For ellipsometrical samples control, a configuration of rotating analyzer was employed (Fig. 1). As a radiation source S^* we used a LED with main wavelength $\lambda = 625$ nm and spectral FWHM $\Delta\lambda = 10$ nm. The polarization plane of incident wave was oriented at 45° in relation to the incident plane (p-plane). For each required beam incident angle θ onto the sample intensity of reflected beam was measured while rotating analyzer A. Using these data, control software reproduces the shape of the reflected light polarization ellipse and computes the angular dependencies of the azimuth of the restored linear polarization $\psi(\theta)$ and the phase shift between p- and s-components $\Delta(\theta)$.

During ellipsometric measurements, the samples were irradiated

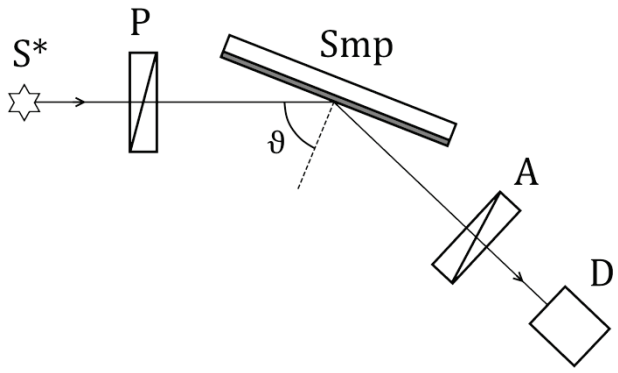

Fig. 1. Ellipsometer configuration of the experimental installation (external reflection). S^*—radiation source, P—polarizer, Smp—sample, A—analyzer, D—radiation detector.

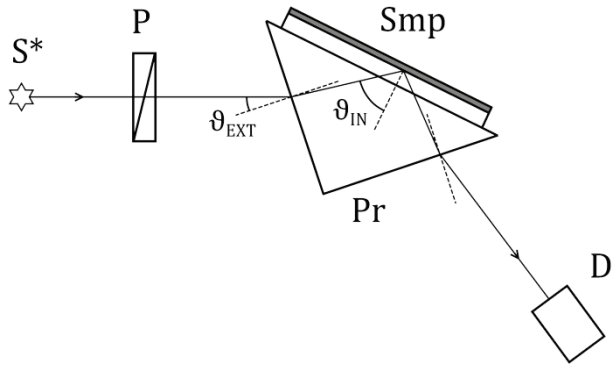

Fig. 2. Experimental setup configuration to record SPR-curves (internal reflection). S*—radiation source, P – polarizer, Pr—prism, Smp—sample, D—radiation detector.

from the side of the deposited thin films.

To excite surface plasmons in metal films we used geometry of experiment typically known as Kretschmann configuration. Figure 2 illustrates it schematically. Linearly polarized light with polarization oriented along the *p*-plane falls onto a glass prism at a certain angle θ_{EXT}. The prism has a cross-sectional shape in the form of a rectangular isthopedic triangle, and its refractive index is $n = 1.511$ at $\lambda = 625$ nm. Under normal circumstances, the ray is completely reflected from the hypotenuse face of the prism, and then goes outside and is recorded by the photodetector.

In the experiment, a sample is placed on the hypotenuse face, so that its glass substrate becomes like a continuation of the prism medium. To provide an optical contact between the prism and sample substrate we employed Vaseline oil (oleum vaselini) as an immersion. Its refractive index amounts $n = 1.464$ in selected spectral range. So, the ray is reflected from heterostructure inside of sample substrate. At certain incident angles, favourable conditions are created for the occurrence of SPR, and a portion of light wave energy pass to the sample. Sequentially positioning the prism with the sample at required angles θ_{EXT}, the mentioned apparatus records the dependency of output light intensity on the angle of external incidence θ_{EXT}.

3. THEORETICAL MODEL OF HETEROSTRUCTURES OPTICAL PROPERTIES

The program for computing light propagation in multilayer structures was created on the base of matrix method. To calculate the azimuth of restored linear polarization ψ and the phase shift between *p*- and *s*-

components of light, reflected from such structures, we had employed electromagnetic radiation theory described in [9]. Determination of reflection, transmission and absorption coefficients of such a system in terms of electromagnetic theory is reduced to the boundary value problem solution. It is necessary to found the stationary amplitudes of the electric and magnetic fields strength vectors at all boundaries of the multilayer system, taking into account interference phenomena. The required energy ratios and phase changes in the final calculation are written through the corresponding field vectors.

It can be assumed that the incident light is described by a plane wave; it is linearly polarized and monochromatic. Concerning the investigated thin-film structure, it can be assumed that it consists of infinitely wide planar-parallel layers, homogeneous and isotropic. The interfaces are considered as ideal. Then the optical properties of each such layer are fully described by a complex index of refraction $N_j = n_j - ik_j$ and geometrical thickness d_j. The numbering is selected, starting with the upper oxide layer for the external reflection, or starting with the lower intermediate Cr layer for the internal reflection.

First, according to the recurring formulas given in [9], which are convenient to write in the form of matrix equations, complex vectors of tension are calculated on boundaries of sample media. As a result, the reflection coefficient and phase change of the electrical component of the light wave are determined as follows:

$$R = \left| \frac{E_{0^-}^{(r)}}{E_{0^-}^{(t)}} \right|^2 , \tag{1}$$

$$\rho = \arg \left[\frac{E_{0^-}^{(r)}}{E_{0^-}^{(t)}} \right], \tag{2}$$

where $E_{0^-}^{(t)}$ and $E_{0^-}^{(r)}$ are the falling on and the reflected from the first boundary waves amplitudes, respectively.

To find the ellipsometric parameters ψ and Δ, one needs to make such calculations for *p*- and *s*-waves. Then

$$\psi = \operatorname{arctg} \left(\left| \frac{\left(E_{0^-}^{(r)}\right)_p}{\left(E_{0^-}^{(r)}\right)_s} \right| \right), \tag{3}$$

$$\Delta = \pi - \left| \arg \left[\frac{\left(E_{0^-}^{(r)}\right)_p}{\left(E_{0^-}^{(r)}\right)_s} \right] \right| . \tag{4}$$

To calculate the angle of incidence of a beam in a prism, the follow-

ing formula derived from geometric considerations is used:

$$\vartheta_{IN} = \arcsin\left[\frac{n_1}{n_3}\sin\left(90^\circ + \arcsin\left[\frac{n_0}{n_1}\sin\left(\vartheta_{EXT}\right)\right] - \frac{\gamma}{2}\right)\right], \tag{5}$$

where γ is the main angle of the prism (90° in our case).

Light intensity at the system output is described as

$$I_0' = I_0 T_{01} T_{12} T_{23} R_{IN} T_{32} T_{21} T_{10} = \left(T_{01} T_{12} T_{23}\right)^2 R_{IN}, \tag{6}$$

where T_{ij} are the power transmission coefficients, determined from Fresnel's formulae. In these two equations index 0 corresponds to the ambient (air), 1—to the prism, 2—to the immersion, and 3—to the sample substrate.

So we obtain an SPR-curve $R_{IN}(\theta_{IN})$, and the measured external reflection coefficients $R_{EXT}(\theta_{EXT})$ are adjusted to obtain the internal reflection coefficient $R_{IN}(\theta_{IN})$. It should be noted that when turning the prism (Fig. 2) during the experiment, the light pattern moves along the surface of the specimen. Avoiding this would be an additional prism shifting along the plane of its mirror symmetry during positioning, but such a technique in our experiment was not used. Therefore, the prism with the sample was placed on the installation rotary table a bit decentralized in order to minimize probe point drift along heterostructure surface. The structure of each layer in the samples was been assumed to be homogeneous throughout their surface.

4. RESULTS AND DISCUSSION

In order to determine the optical constants of each of the thin films, the heterostructures were examined for the angular dependences of their ellipsometric parameters $\psi(\theta)$ and $\Delta(\theta)$ at external reflection [8]. According to the above mentioned methodology, theoretical calculations of the corresponding dependences have been carried out and the optimal values of the refractive index n and extinction coefficient k were been selected, which give the minimum deviations from the experimental data. To simplify the task, we regarded optical constants n and k of thin Cr layer, as well as HfO_2 and MgF_2 to be known values (see Table 2), because their variation, as it turned out, weakly affects the shape of the curves $\psi(\theta)$ and $\Delta(\theta)$.

The experimental data obtained, except for the dependence $\psi(\theta)$ for sample 2, are in good agreement with the results of the calculation according to the proposed theoretical model. The experimental and theoretical dependences $\Delta(\theta)$ coincide with the slight deviation of the extinction coefficients of thin metal layers (Au, Ag, Cu) from the litera-

TABLE 2. Literary data on the optical constants of used materials at $\lambda = 625$ nm.

Material	n	k	Reference
Ag	0.050	4.251	[10]
Au	0.153	3.522	[10]
Cu	0.113	3.484	[10]
Cr	3.155	3.308	[11]
HfO_2	2.107	0*	[12]
MgF_2	1.421	0*	[13]

*Approximately accepted by us.

ture data for bulk metals. At the same time, the corresponding dependences $\psi(\theta)$ are qualitatively similar, however, their complete coincidence can only be achieved by considerable changing the optical parameters (n and k) of the layers. Then this causes a distinction between the corresponding dependences $\Delta(\theta)$. That's why the optical parameters of the metal films were resolved to vary in two approaches: (*a*) for the best coincidence for a certain sample of two comparable dependences $\Delta(\theta)$; (*b*) for the smallest deviations in the dependence pairs both by the value of $\Delta(\theta)$ and $\psi(\theta)$ for a certain sample. As a typical example Fig. 3 illustrates these approaches for sample 8. The results of corresponding final choice of the optical constants n and k of individual layers values for the samples investigated are given in Table 1.

From Fig. 3 it is obvious that the inverse problem of ellipsometry solution by criterion (*a*) is more reliable than criterion (*b*), since the displacement of the experimental curve $\psi(\theta)$ along the vertical while the curves $\Delta(\theta)$ coincide can be explained by the effects of light scattering in the sample, which depend on the radiation polarization state. Thus, the displacement ψ vertically by 1° corresponds to approximately 4% difference in the scattering between p- and s-components of polarized light.

For each sample, the angular dependence of internal reflection coefficient $R_{IN}(\theta_{IN})$ of p-polarized light in Kretchman's geometry was also measured. The corresponding graphs are presented in Fig. 4. These dependences demonstrate a good qualitative agreement of experimental and theoretical results. A common peculiarity of the experimental curves is the smaller amplitude of the change in the values of R_{IN} and their smoothened form compared to the theoretical curves. This behaviour can be explained by the fact that the actual thickness of the layers is not exactly the same throughout the film surface, since at a height each layer contains only about 10–100 atoms (and even less for Cr adhesive layer). Then, the interference conditions for each point on the

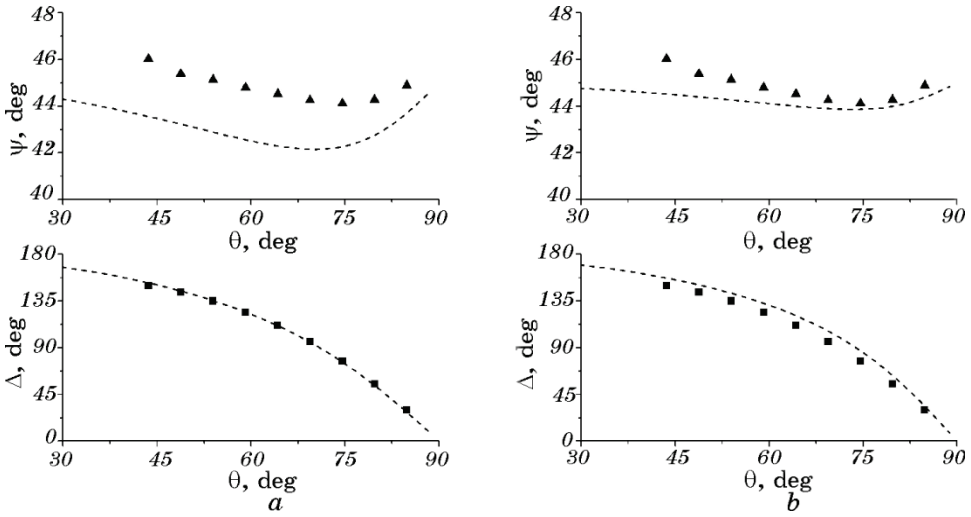

Fig. 3. Combination of experimental (symbols) and theoretical (dashed curves) dependences $\psi(\theta)$ and $\Delta(\theta)$ at external reflection for the sample 8 in approaches (*a*) only for $\Delta(\theta)$, (*b*) $\psi(\theta)$, and simultaneous variations for $\Delta(\theta)$.

sample surface, and hence the inverse problem solution, will differ a bit. Therefore, the resulting reflection curve can be represented by a sum of the corresponding curves for individual fragments of the film, the thickness of which is somewhat different. It is natural to expect that their composition will lead to a distortion observed in the experiment.

It should be also noted that for the sample 7 the calculated dependences $\psi(\theta)$ and $\Delta(\theta)$ at external reflection coincide with the experimental ones significantly better. This may be caused by the fact that this specimen has a thicker adhesion layer Cr (3 nm) than all others. Then, due to the chrome layer, irregularities on glass substrate are smoothed better and a more flat interface for the next layer of Cu, sputtered above, is formed. Therefore, the interference conditions for light in this layer are less disturbed, which results in more agreement between the experimental ellipsometric parameters ψ and Δ and the results of their theoretical calculations in the approaches of both (*a*) and (*b*) of the model proposed. More rigorous conclusions about the role of the Cr layer could be made, having in addition such heterostructures without this layer. But for technological reasons, their fabrication is beside the purpose.

Using the results for the reflection coefficient of the *p*-polarized wave at SPR excitation, optical characteristics of the layers of materials from which these multilayered structures are composed are estimated. To do this, the parameters n and k of the metallic layers were

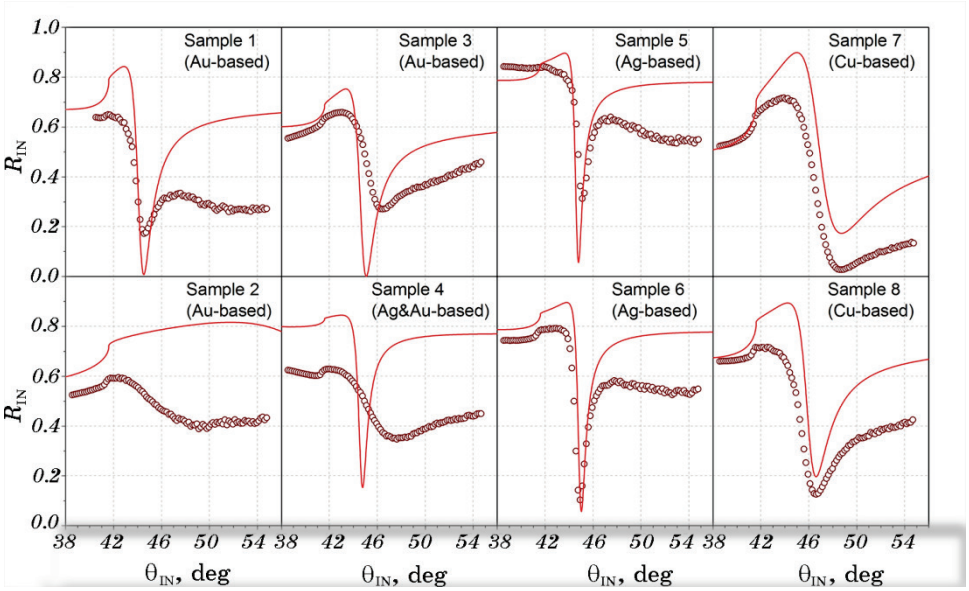

Fig. 4. Experimental (circles) and theoretical (solid lines) angular dependences of the internal reflection coefficient $R_{IN}(\theta_{IN})$ of the samples investigated.

chosen, in which the theoretically calculated angular position of the plasmon minimum of each sample coincided with the position of the appropriate minimum on the experimental curve. This optimality criterion is satisfied ambiguously, since there is no single pair of such optical parameters n and k. Therefore, it is possible to select only the limits of the intervals of their possible values. The results of such optical constants selection are also given in Table 1. Their difference from the literary data is determined by the same factors that influence the form of SPR-curves. Optical parameters n and k of real thin films are determined by their structure, and depend on the mode of film deposition, its thickness, crystalline defects, further annealing. Probably, a more accurate estimation of optical parameters will be possible when improving the theoretical model, which would take into account in a certain way the random deviation of the thickness of the film from the average value at different parts of the surface. It should be noted that the greatest influence on the modelling results is the variation of the optical thickness of the upper dielectric layer (HfO_2), which indicates its significant role in the resonance curve formation.

Among the calculations results, the reflection coefficient $R_{IN}(\theta_{IN})$ of sample 2 behaviour attracts special attention. It cannot be explained without significant change in the optical thickness (nd, n—refractive index, d—thickness) of HfO_2 layer. A satisfactory coincidence of theoretical and experimental values can be achieved either by decreasing

the thickness of the layer from 30 to 13 nm, or by decreasing the refractive index of HfO_2 from 2.107 to 1.350.

Relying on the good agreement between theoretical and experimental data for both ellipsometric measurements and measurements of $R_{IN}(\theta_{IN})$, the proposed theoretical model was used to estimate the efficiency level of these structures when used as plasmonic sensors. As is well known [2], such sensors function on the principle of registering the SPR-curve angular position, therefore, for each sample, the angular position of the minimum of the $R_{IN}(\theta_{IN})$ is numerically calculated as a function of the refractive index of the medium that is in contact with the upper (oxide) surface sensor. These dependencies are shown in Fig. 5.

From Figure 5 it is evident that the difference between them is insignificant, except for the curve for sample 2. The dependences for copper-based samples (sensors) 7 and 8 stand out somewhat by shifting upwards by ≈4.9° and ≈2.6°, respectively. This leads to a slight decrease in the maximum possible in the diagnosis of the refractive index of the controlled substance that can be captured by such a sensor. The curve inclination in Fig. 5 defines sensor sensitivity to change the refractive index. For the all samples, it is almost identical and amounts ~100 deg/RIU (Refractive Index Unit) in the vicinity of n = 1.20. It should be noted that a certain increase in the sensitivity of sensors

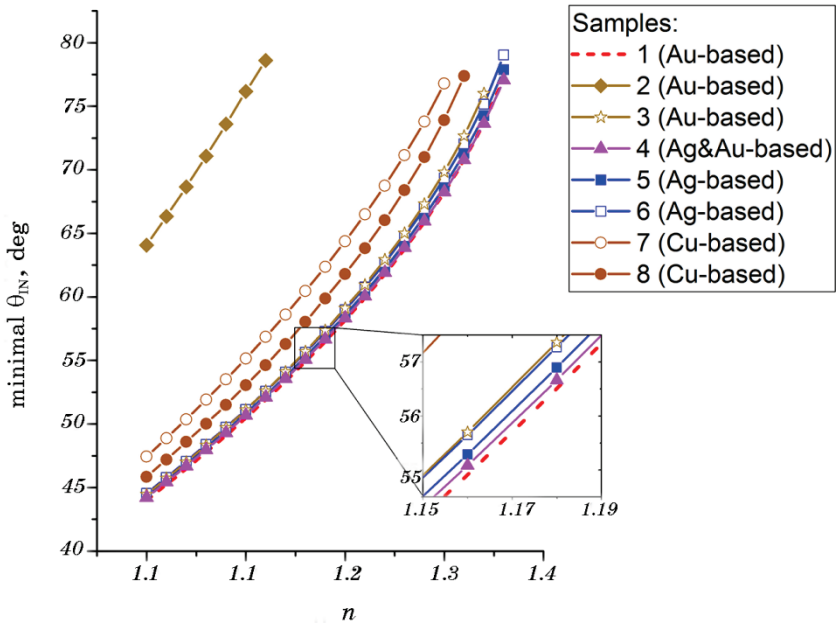

Fig. 5. The dependences of SPR-curve minimum angular positions *versus* an analyte refractive index n value.

with the increase of the refractive index (≈ 30 deg/RIU the vicinity of $n = 1.30$) due to a growth of the inclination of the corresponding curves.

5. CONCLUSIONS

The intermediate Cr layer probably not only implements a function of adhesive material in a sensor based on plasmon excitation, but also provides a flat interface formation for the next heterostructure layer by filling in the inequalities of the glass substrate surface. This improves the interference conditions in the next layer which leads to surface plasmon resonance curve FWHM narrowing and increases the efficiency of the sensor being produced.

It was established that the optical thickness of the protective HfO_2 layer on the top of Au film significantly influences the shape of the surface plasmon resonance curve, and therefore the requirements for the homogeneity of this layer during deposition process should be essentially high. The resonance curve minimum shifts to higher angles of incidence whereas the optical thickness of oxide layer rises. Then the range of refractive index available for diagnosis is narrowed. Similar assertions for Ag and Cu films derive from theoretical modelling, but they require experimental verification to be ultimate.

It was shown that sensitivity of plasmon sensors based on Au, either Ag and Cu to the deviation of the controlled substance refractive index slightly increases while refractive index rises and practically does not depend on the type of a metal chosen for sensor formation.

REFERENCES

1. B. Liedberg, C. Nylander, and I. Lunström, *Sens. Actuators*. **4**: 299 (1983).
2. J. Homola, S. S. Yee, and G. Gauglitz, *Sens. Actuators B*, **54**: 3 (1999).
3. J. N. Anker, W. P. Hall, O. Lyandres, N. C. Shah, J. Zhao, and R. P. Van Duyne, *Nat. Mater.*, **7**: 442 (2008).
4. P. R. West, S. Ishii, G. V. Naik, N. K. Emani, V. M. Shalaev, and A. Boltasseva, *Laser & Photonics Reviews*, **4**: 795 (2010).
5. M. Futamata, *Appl. Opt.*, **36**: 364 (1997).
6. V. G. Kravets, R. Jalil, Y.-J. Kim, D. Ansell, D. E. Aznakayeva, B. Thackray, L. Britnell, B. D. Belle, F. Withers, I. P. Radko, Z. Han, S. I. Bozhevolnyi, K. S. Novoselov, A. K. Geim, and A. N. Grigorenko, *Sci. Rep.*, **4** (2014).
7. V. G. Kravets, A. K. Petford-Long, and A. F. Kravets, *J. Appl. Phys.*, **87**: 1762 (2000).
8. A. L. Yampolskiy, O. V. Makarenko, L. V. Poperenko, and V. O. Lysiuk, *Quantum Electronics and Optoelectronics*, **21**: 412 (2018).
9. *Physics of Thin Films: Advances in Research and Development* (Ed. G. Hass) (New York and London: Academic Press: 1963).

10. K. M. McPeak, S. V. Jayanti, S. J. P. Kress, S. Meyer, S. Iotti, A. Rossinelli, and D. J. Norris, *ACS Photonics*, **2**: 326 (2015).
11. P. Johnson and R. Christy, *Phys. Rev. B*, **9**: 5056 (1974).
12. D. L. Wood, K. Nassau, T. Y. Kometani, and D. L. Nash, *Appl. Opt.*, **29**: 604 (1990).
13. L. V. Rodríguez-de Marcos, J. I. Larruquert, J. A. Méndez, and J. A. Aznárez, *Opt. Mat. Express.*, **7**: 989 (2017).